Journal of Alloys and Compounds 473 (2009) 363–367

Contents lists available at ScienceDirect

Journal of Alloys and Compounds

journal homepage: www.elsevier.com/locate/jallcom

Crystallization of α-Fe phase in amorphous $Fe_{81}B_{13}Si_4C_2$ alloy

D.M. Minić[a,*], A. Maričić[b], B. Adnađević[a]

[a] Faculty of Physical Chemistry, University of Belgrade, Studentski trg 12, 11 000 Belgrade, Serbia
[b] Technical Faculty Čačak, University in Kragujevac, Serbia

ARTICLE INFO

Article history:
Received 12 April 2008
Received in revised form 20 May 2008
Accepted 23 May 2008
Available online 3 July 2008

Keywords:
Amorphous materials
Metallic glasses
Metals and alloys
Phase transition
Thermal analysis

ABSTRACT

The crystallization kinetics of α-Fe from the amorphous $Fe_{81}B_{13}Si_4C_2$ alloy was investigated by DSC and XRD methods. The kinetic parameters ($\ln A$, E_a) of the investigated process were determined using Kissinger's as well as isoconversional (model-free) method. Based on the results of DSC and XRD analysis and calculated crystallization parameters ($n = 4$; $m = 3$) it was concluded that primary crystallization of α-Fe phase in amorphous matrix occurs through the bulk nucleation and three-dimensional growth of nuclei growing with constant rate.

1. Introduction

The amorphous alloys (metallic glasses) are a relatively new class of materials with a specific combination of properties which are very interesting from technological point of view. These materials are characterized by structure with absence of the distant order atom arrangement and characterized by high degree of anisotropy of physical properties [1,2].

The amorphous state of matter is, however, structurally and thermodynamically unstable and very susceptible to partial or complete crystallization during thermal treatment or non-isothermal compacting [3]. The crucial limitation with respect to using metallic glasses for high temperature applications arises from their restricted thermal stability. The onset of exothermic crystallization upon crossing the stability domain of the glassy state results in the formation of highly stable, but brittle intermetallic compounds, which renders these alloys useful only once. Further, for amorphous alloys that exhibit excellent magnetic properties the crystallization represents the limit at which these properties begin to deteriorate. For the case alloys that exhibit excellent magnetic properties in the two-phase nanocrystal-amorphous matrix structure, control of the crystallization kinetics allows the ability to tailor the desired structure. The latter imposes the knowledge of alloys stability in a broad range of temperature due to different crystallization processes which occur during its annealing [4].

Among these materials the amorphous alloys of Fe and B, have been very interesting because of their soft ferromagnetic properties with a high saturation magnetic flux density. These alloys are applicable in a variety of devices, including transformers, magnetic tapes and recorder heads [5–7]. It was determined that the Curie temperature of alloys increases slightly on replacement of boron by silicon [8]. This results in a sharp increase of relatively constant room-temperature saturation magnetization extending from $Fe_{80}B_{20}$ to $Fe_{82}B_{12}Si_6$. The multicomponent alloys are generally easier to prepare in the amorphous state than the binary ones. So, it was concluded that the crystallization temperature increases with increase of content of silicon and decrease of contents of iron and boron. Thus for the highest saturation magnetization alloy combined with ease of preparation, stability, and lowest losses, the multicomponent alloys $Fe_{81}B_{17}Si_2$ and $Fe_{82}B_{12}Si_6$ are preferred [8]. It was also shown that the soft magnetic properties of Fe–B alloy are improved by a decrease of the α-Fe grain size from 20 to 10 nm [9].

The crystallization of amorphous alloys upon heating can be performed in several ways. In calorimetric measurements, two basic methods are in use, isothermal and non-isothermal. The results of crystallization process can be considered in terms of several theoretical models [10]. The investigation of kinetics of the crystallization showed that the crystallization process of amorphous $Fe_{83}B_{17}$ is governed by a bulk growth in two dimensions ($n = 2$) [11]. However, the investigation of the crystallization kinetics of

* Corresponding author. Tel.: +381 11 333 6689; fax: +381 11 2187 133.
E-mail address: dminic@ffh.bg.ac.yu (D.M. Minić).

0925-8388/$ – see front matter © 2008 Elsevier B.V. All rights reserved.
doi:10.1016/j.jallcom.2008.05.087

amorphous alloy $Fe_{81}B_{13.5}Si_{3.5}C_2$ showed three exothermal peaks on DSC curves showing that the crystallization process includes formation more than one phase. The isothermal annealing at $T > 780$ K leads to the appearing of crystalline phases α-Fe and Fe_2B_3 in the mentioned alloy but the further increase of annealed temperature leads to appearance of metastable γ-Fe phase [12,13]. It was shown the diffusion controlled growth particles of appreciable initial volume and three-dimension growth of small particles [13]. The values of Avrami exponents ($n_I = 1.6$ and $n_{II} = 2.0$) calculated for $Fe_{78}B_{13}Si_9$ are characteristic for the diffusion-controlled growth of small particles with decreasing nucleation rate. Atomic rearrangement and amorphous-to-crystalline transformations during isothermal annealing have been investigated by Mössbauer spectroscopy [14]. It was shown that rearrangement in the amorphous state consists of two processes depending on the annealing temperature. The first process is attributed to the enhancement of the short-range order and the second one to the atomic rearrangement leading to crystallization. The crystallization was found to consist of at least two steps giving as the final crystalline products Fe_2B and Fe_3B.

Having in mind the influence of thermal stability and microstructure on the physicochemical properties of amorphous alloys as well as shown differences in kinetics of crystallization, in this work, the crystallization process of α-Fe from the $Fe_{81}B_{13}Si_4C_2$ alloy was investigated in detail from the kinetically point of view by using DSC and X-ray analysis.

2. Experimental procedure

The ribbon-shaped samples of $Fe_{81}B_{13}Si_4C_2$ amorphous alloy were obtained by using the standard procedure of rapid quenching of the melt on a rotating disc (melt-spinning). The obtained ribbon was 2 cm wide and 35 μm thick.

The crystallization process was investigated by the differential scanning calorimetry (DSC) in a nitrogen atmosphere using SHIMADZU DSC-50 analyzer. In this case, samples weighting several milligrams were heated in the DSC cell from the room temperature to 650 °C in a stream of nitrogen with nitrogen flowing at a rate of 20 mL min^{-1} and at the heating rates of 5, 10, 20 and 30 K min^{-1}.

In order to investigate structural transformations by X-ray diffraction, the samples of amorphous alloy $Fe_{81}B_{13}Si_4C_2$ annealed at the different temperatures (20, 200, 300, 400, 440, 460, 500, 550, 600, 700 and 830 °C) in a stream of nitrogen during 30 min. Then the X-ray powder diffraction (XRD) patterns were recorded on a Philips PW-1710 automated diffractometer using a Cu tube operated at 40 kV and 30 mA. The instrument was equipped with a diffracted beam curved graphite monochromator and Xe-filled proportional counter. For the routine characterization diffraction data was collected in the range of 2θ Bragg angles (4–100° counting for 0.1 s). Silicon powder was used as an external standard for calibration of a diffractometer. All XRD measurements were done with solid samples in a form of ribbon at ambient temperature.

3. The methods used to evaluate the kinetic parameters of the investigated process

All kinetic studies assume that the isothermal rate of conversion $d\alpha/dt$, is a linear function of the temperature-dependent reaction rate constant, $k(T)$, and a temperature-independent function of the conversion, $f(\alpha)$ [15]:

$$\frac{d\alpha}{dt} = k(T)f(\alpha), \tag{1}$$

where α is the fractional extent of reaction, t is the time and the function $f(\alpha)$ depends on the particular crystallization mechanism.

According to Arrhenius's equation:

$$k(T) = A\exp\left(-\frac{E_a}{RT}\right), \tag{2}$$

where A is the pre-exponential factor, that is assumed to be independent of temperature, E_a the apparent activation energy, T the absolute temperature and R is the gas constant, so the rate of conversion is

$$\frac{d\alpha}{dt} = A\ \exp\left(-\frac{E_a}{RT}\right)f(\alpha). \tag{3}$$

For non-isothermal measurements at constant heating rate $\beta = dT/dt$, t is the time, Eq. (3) transforms to

$$\beta\frac{d\alpha}{dT} = A\ \exp\left(-\frac{E_a}{RT}\right)f(\alpha), \tag{4}$$

where $d\alpha/dt \equiv \beta(d\alpha/dT)$.

The integral form of the reaction model can be obtained by integration of Eq. (4):

$$g(\alpha) = \int_0^\alpha \frac{d\alpha}{f(\alpha)} = \frac{AE_a}{R\beta}p(x) \tag{5}$$

where $p(x)$ is the temperature integral for $x = E_a/RT$ which does not have analytical solution.

The apparent activation energy E_a can be calculated by various methods. The Kissinger's method allows the calculation of apparent activation energy from a point T_p which is the temperature at the maximum DSC curve for different rates of heating [16]. Since the maximum rate of investigated process occurs when $(d\alpha/dt)$ is 0, differentiation of Eq. (4) having in mind the general equation enabling the analysis of conversion kinetics for nucleation and growth of particles of new phase proposed by Avrami in the form $f(\alpha) = (1-\alpha)^n$, where n is the apparent reaction order, Kissinger's relation was obtained:

$$\ln\left(\frac{\beta}{T_p^2}\right) = \ln\left(\frac{AR}{E_a}\right) - \frac{E_a}{RT_p}. \tag{6}$$

The second used method is rate-isoconversion method proposed by Friedman [17]. The basic assumption of method is that the reaction rate at a constant conversion value is only a function of temperature. This premise supposes possibility of determination of kinetic parameters, $E_{a,\alpha}$ and A_α, for each value of α over the entire reaction range. The method does not require any assumption on the $f(\alpha)$ and it is also known as "model-free method". The rate-isoconversion method was based on Eq. (4) in the logarithmic form:

$$\ln\left[\beta_i\left(\frac{d\alpha}{dT}\right)_{\alpha,i}\right] = \ln[A_\alpha f(\alpha)] - \frac{E_a}{RT_{\alpha,i}}, \tag{7}$$

where a subscript α designates values related to a given conversion, and i is a number of the non-isothermal experiment conducted at the heating rate β_i. By plotting $\ln[\beta_i(d\alpha/dT)_{\alpha,i}]$ against $1/T_{\alpha,i}$, the value of the $-E_a/R$ for a given value of α can be directly obtained.

4. Results and discussion

Typical DSC curve obtained during heating and cooling cycle is presented in Fig. 1.

DSC curve (Fig. 1) involves series of endo- and exo-peaks indicating a stepwise process of structural stabilization of alloy in the temperature range 200–560 °C. A broad exo-peak, indicated as low temperature peak (T_k^1) in temperature range 200–400 °C, is followed by endothermic hump (temperature of glass transition T_g) and a short supercooled liquid region before sharp exothermic crystallization peak (T_k) in temperature range 500–560 °C (Fig. 2).

All values of initial (T_i), maximal (T_p) and final temperature (T_f) for both exo-peaks are shifted to higher values with increasing heating rate indicating the presence of kinetic effects. The overall apparent activation energy for crystallization process, under linear heating condition was calculated by the Kissinger's peak

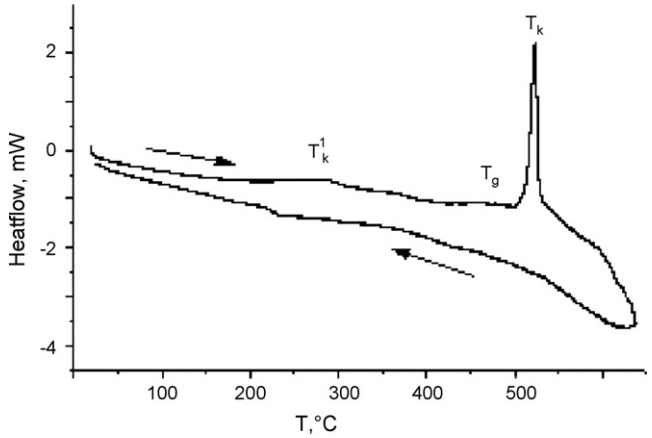

Fig. 1. DSC curve of heating and cooling cycle; heating rate 10 °C/min.

method [16]. The values of peak temperatures together with values of kinetic parameters (E_a and $\ln A$) calculated by Kissinger's method and the symmetry factors (SFs) are given in Table 1.

The changes of structure in the temperature range (20–830 °C) were followed by X-ray diffraction method on as prepared as well as alloy annealed at different temperatures (Fig. 3).

X-ray diffraction pattern of the as-quenched ribbon shows only a broad halo at 2θ range of 40–55° suggesting an amorphous (glassy) structure. Diffraction patterns of alloy annealed at the temperatures of $T \leq 460$ °C contain the same halo as well as the original sample but also contain one sharp peak at $2\theta = 83.2°$ indicating presence of structural deformed crystal phase as consequence of ordering Fe-clusters already present in starting alloy. Increase of annealed temperature results in a decrease of intensity of this peak and appearance the new sharp peak at $2\theta = 45.6°$ whose height increases with an increase of annealing temperature. The increase

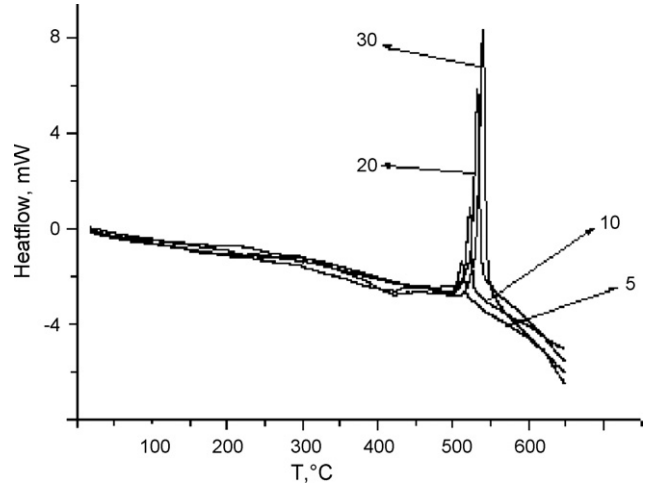

Fig. 2. DSC curves at different heating rates.

Table 1
The values of T_p and kinetic parameters of crystallization of amorphous $Fe_{81}B_{13}Si_4C_2$ alloy upon continuous heating at different heating rates

β (K/min)	T_p (K)	E_a (kJ mol^{-1})	$\ln A$	SF
5	785	351.2	52.75	0.98
10	793			0.98
20	804			0.98
30	811			0.98

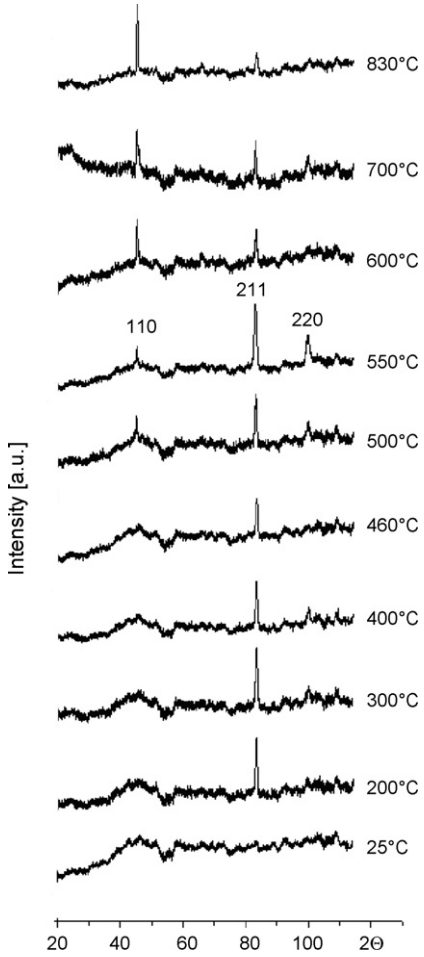

Fig. 3. XRD patterns for as quenched and annealed alloy.

of intensity of that peak as well as a decrease of its half width indicates the increase of crystallinity of alloy. This shows that at higher temperature (above 500 °C) the process of crystallization occurs. Thoroughly studying of diffractograms by the comparative semi-qualitative analysis of annealed alloy (JCPDS-PDF 03-065-4899) gives evidence for the presence of α-Fe crystallization in annealed alloy. The disarranged ratio of peak intensities of diffractions lines indicates very deformed crystal structure whose disorder disappears with the increase of temperature of annealing according the ratio of height of diffraction peaks.

The detailed crystallization kinetics of α-Fe in the amorphous alloy was studied by differential scanning calorimetry in temperature range of 500–560 °C. The volume fraction (or degree of conversion, α) of the sample transformed into crystalline phase during the crystallization process has been obtained from the DSC curve as a function of temperature (T). The volume fraction crystallized, α, at any temperature T is given as $\alpha = S_T/S$, where S is the total area of the exotherm between the temperature T_i, where the crystallization is just beginning and the temperature T_f, where the crystallization is completed, and S_T is the area between the initial temperature and a generic temperature, T, ranging between T_i and T_f [17]. The plots of α versus T at different heating rates for the considered crystallization process are shown in Fig. 4.

The sigmoid shape of fractional conversion curves in Fig. 4 indicates crystallization in bulk amorphous material excluding the surface crystallization. For all heating rates, these curves show a slow initial period corresponding to dominant process of nucleation with increasing rate caused by increase of specific area of

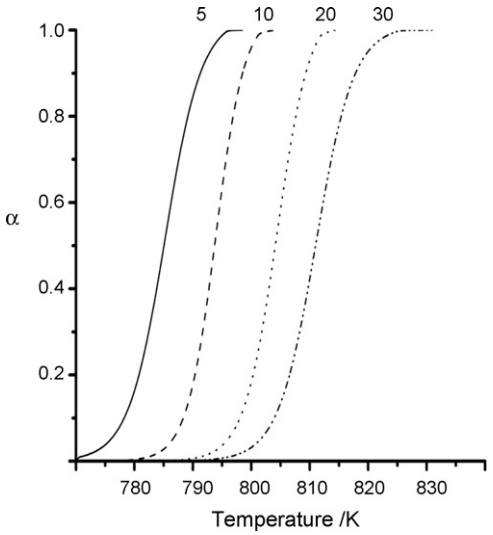

Fig. 4. Fractional conversion (α) as a function of temperature (T) for the crystallization alloy at different heating rates (5, 10, 20 and 30 K min^{-1}).

nuclei. The following part of saturation is the consequence of attaching nuclei causing the decrease of surface area.

It can be observed that the apparent activation energy for the considered crystallization process is practically constant in the $0.2 \leq \alpha \leq 0.7$ range, Fig. 5, indicating the existence of a single-step reaction [15,18]. The average value of apparent activation energy was determined as $E_a = 356.5 \pm 5.5$ kJ mol^{-1}.

The activation energy of crystallization process proceeding through formation of nuclei and their growth, according to opinion of some researches, has no physical meaning but only empirical character and practically establishes only the dependence of the rate of conversion on temperature. This energy can be spent, not only for overcoming the activation barrier but also mainly for its downturn due to cooperative displacement plenty of atoms. Finely, the crystallization of amorphous alloys is a very complicated process accompanied by nucleation and growth of various crystal phases under continuously varied conditions of chemicals surroundings in a zone of conversion. Obviously, such a process occurs not only with the single value of activation energy and not by formation of a single configuration of activated complex. In practice, with the multitude of probable ways of conversions, only those mechanisms and activated complexes of the crystallization process will be realized that are the most probable at a given temperature. Any change of crystallization conditions, such as heating rate, can result in a change of the mechanism and main activation complex of the crystallization process. Thus high values of activation energy of crystallization of amorphous alloys, first of all, indicates that a lot of atoms participate in an elementary act of structure reorganization, as well as high complexity of these processes.

For the preliminary determination of kinetic model of the investigated crystallization process, Dollimore's method was used [19–21]. This model is based on the "sharpness" of initial and final temperature of the differential rate curves as well as on its asymmetry. From the result of the theoretical considerations it is apparent that the "sharpness" of the initial and final temperatures is caused by kinetic factors, and especially by the mechanism of process. Certain kinetic models lead to an asymptotic or diffuse departure from the base line in a differential form thermal curve, while the others produce a very sharp approach to the final plateau. According to these parameters the authors listed three different types of kinetic mechanisms [21]. The investigation of these parameters that describe geometry and asymmetry of the differential rate

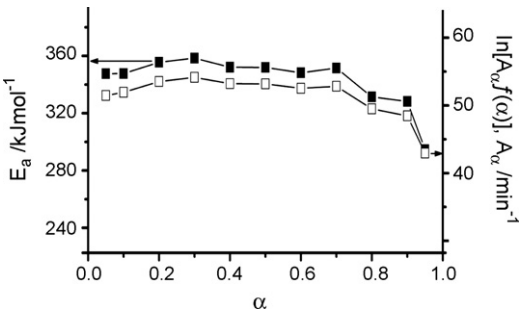

Fig. 5. The apparent activation energy (E_a) and intercept (ln[$A_\alpha f(\alpha)$]) plotted as a function of fractional conversion (α).

curves it can be very simple to indicate the probable kinetic mechanism expressed as $f(\alpha)$. So, when the crystallization process is not complex the qualitative approach to kinetic may be obtained using parameters such as α_{max} or $(d\alpha/dt)_{max}$, the shape of the initial and final temperatures as well as peak temperature (T_p), half-width from differential rate curves.

In our case, Dollimore's procedure was applied on the conversion and differential rate curves whose asymmetry is observed between T_i and T_f for the differential rate curves (Fig. 6). The others parameters such as the conversion at the rate of maximum crystallization, α_{max}, peak temperature, T_p, at $(d\alpha/dt)_{max}$, and the ratio ΔLoT/ΔHiT (shape factor), which is the ratio between the low-temperature at half-width and high-temperature at half-width of the differential rate curve peak, are presented in Table 2.

The dependence of $d\alpha/dt$ versus T at different heating rates for the investigated crystallization process of α-Fe in the amorphous $Fe_{81}B_{13}Si_4C_2$ alloy is shown in Fig. 6. It is clearly seen that the position of the broadening exotherm, which is connected with the crystallization was shifted toward higher temperature with

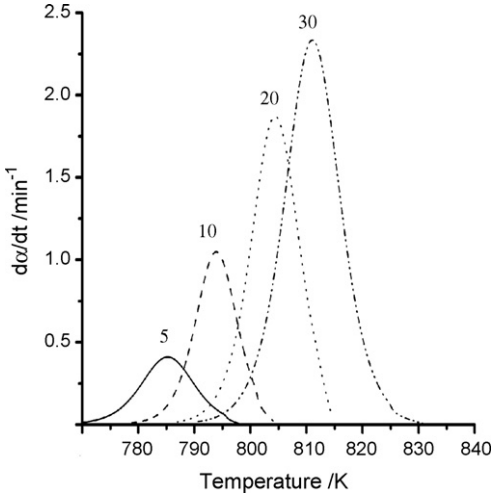

Fig. 6. Differential rate curves ($d\alpha/dt$ vs. T) for different heating rates (β = 5, 10, 20 and 30 K min^{-1}).

Table 2
Parameters describing the asymmetry DSC curves of crystallization α-Fe phase in amorphous $Fe_{81}B_{13}Si_4C_2$ alloy

β (K/min)	α_{max}	ΔLoT/ΔHiT	Half-width (K)	T_i	T_f
5	0.51	1.0	9.5	Sharp	Sharp
10	0.53	1.0	9.5	Sharp	Sharp
20	0.53	0.9	10.0	Sharp	Sharp
30	0.55	0.8	11.0	Sharp	Sharp

Table 3
Values of constants n and m for different crystallization mechanisms

Mechanism	n	m
Bulk nucleation		
Three-dimensional growth	4	3
Two-dimensional growth	3	2
One-dimensional growth	2	1
Surface nucleation	1	1

Table 4
The values of n values at three temperatures

Temperature (K)	n
791	3.92
793	4.08
795	4.07

the increase of the heating rate as well as asymmetry of peaks. This suggests that the crystallization process should not be characterized by a definite critical temperature independent of the heating rate. The determined values of α_{max} for different heating rate were in the range from 0.51 to 0.55. These results indicate that the non-isothermal crystallization mechanism of α-Fe in amorphous $Fe_{81}B_{13}Si_4C_2$ alloy cannot be fully described within the JMA (Johnson–Mehl–Avrami) models (A2, A3 and A4, Group A) which predicated that. Johnson–Mehl–Avrami equation concerning the kinetics of phase transformation (models A1–A4) involving nucleation and growth crystals under isothermal conditions can be used in very limited number of crystallization processes in non-isothermal conditions when the process of nucleation is finished before starting the process of growth of nuclei.

The broadened exothermic peaks almost symmetrical (Fig. 6) indicate the occurrence of the overlapping reactions, probably nucleation and growth of nuclei which occur at same time. Therefore we decided to study further the crystallization kinetics as a whole, as it is a single crystallization peak.

For non-isothermal crystallization, where the volume fraction of crystalline phase α precipitated in glass heated at a uniform heating rate β is related with the activation energy E_a, Matusita et al. proposed the following relation [22–24]:

$$\ln[-\ln(1-\alpha)] = -n\ \ln\beta - \frac{1.052mE_a}{RT} + \text{const}, \quad (8)$$

where m and n are constants having values between 1 and 4 depending on the morphology and kinetics of the growth nuclei (Table 3).

The values of n obtained from the slopes of linear plots $\ln[-\ln(1-\alpha)]$ versus $-\ln\beta$ at different temperatures for considered crystallization process are given in Table 4.

For all considered temperatures, in the limits of experimental errors, the value of n is ≈4.0. From these results follows, that the kinetics of crystallization process is independent from the temperature.

The crystallization exponent n is connected with the number of growth dimensions (m) and the number of nuclei forming stages (s) [22] by the following equation:

$$n = m + s \quad (9)$$

where m is the number of growth dimensions as defined in Table 5, s is the number of the nuclei forming stages ($s=0$ at instantaneously nucleation; $s=1$ at constant nucleation rate and $s>1$ at self-acceleratory nucleation rate).

In order to describe in detail the considered crystallization process, the value of parameter m should be determined from the plot

Table 5
The values of m and n for the different heating rates

β (K/min)	m	s
5	2.84	1.16
10	3.08	0.92
20	3.22	0.78
30	2.84	1.16

of $\ln[-\ln(1-\alpha)]$ because a function of reciprocal temperature is linear with a slope of $1.051(m+1)E_a/R$ using the value of activation energy determined above. The values of parameters m and s obtained at the different heating rates for the investigated crystallization process of α-Fe in $Fe_{81}B_{13}Si_4C_2$ amorphous alloy are given in Table 5.

Based on the obtained values of parameters m and s, at the different heating rates (Table 5), we asserted with high degree of reliability, that the nucleation process of α-Fe occurs within amorphous alloy with a constant rate. The growth of α-Fe crystallites occurs in three effective directions (three-dimensional growth) proceeding with constant nucleation rate.

5. Conclusions

By the annealing of amorphous $Fe_{81}B_{13}Si_4C_2$ alloy at temperatures $T \geq 773$ K, the crystallization process of α-Fe occurs in the bulk of the considered alloy. The nucleation process of α-Fe occurs within the amorphous phase with a constant rate. The growth of α-Fe crystallites is a three-dimensional and occurs with the relatively high value of apparent activation energy of 352.5 ± 5.5 kJ mol^{-1}.

Acknowledgements

The investigation was partially supported by the Ministry of Science and Environmental Protection of Serbia, under the following Projects 142011G and 142025.

References

[1] J.D. Bernal, Nature 185 (1960) 68.
[2] S. Takayma, J. Mater. Sci. 11 (1976) 164.
[3] D.M. Minić, A. Maričić, R.Z. Dimitrijević, M.M. Ristić, J. Alloys Compd. 430 (2007) 242.
[4] U. Koster, U. Herold, in: H.J. Guntherodt, H. Beck (Eds.), Glassy Metals. I. Topics in Applied Physics, vol. 46, Springer, New York, 1981, p. 225.
[5] R.A. Cowley, D. Mck. Paul, W.G. Stirling, S.N. Cowlam, Physica 120B (1983) 373.
[6] N. Cowlam, J. Non-Cryst. Solids 205–207 (1996) 567.
[7] S.D. Kaloshkin, I.A. Tomilin, Thermochim. Acta 280–281 (1996) 303.
[8] F.E. Luborsky, J.J. Becker, J.L. Walter, H.H. Liebermann, IEEE Trans. Magn. 15 (1979) 1146.
[9] T. Ohkubo, H. Kai, D.H. Ping, K. Hono, Y. Hirotsu, Scripta Mater. 44 (2001) 971.
[10] S. Vyazovkin, C.A. Wight, Thermochim. Acta 340–341 (1999) 53.
[11] A.A. Soliman, S. Al-Heniti, A. Al-Hajry, M. Al-Assiri, G. Al-Barakati, Thermochim. Acta 413 (2004) 57.
[12] D.R. dos Santos, D.S. dos Santos, Mater. Res. 4 (2001) 47.
[13] D.R. dos Santos, D.S. dos Santos, J. Non-Cryst. Solids 304 (2002) 56.
[14] N. Segusa, A.H. Morrish, Phys. Rev. B 26 (1982) 305.
[15] S. Vyazovkin, Thermochim. Acta 355 (2000) 155.
[16] H.E. Kissinger, Anal. Chem. 29 (1957) 1702.
[17] H.L. Friedman, J. Polym. Sci. Part C 6 (1964) 183.
[18] J. Opfermann, H.J. Flammersheim, Thermochim. Acta 397 (2003) 1.
[19] D. Dollimore, T.A. Evans, Y.F. Lee, F.W. Wilburn, Thermochim. Acta 188 (1991) 77.
[20] D. Dollimore, T.A. Evans, Y.F. Lee, G.P. Pee, F.W. Wilburn, Thermochim. Acta 196 (1992) 255.
[21] Y.F. Lee, D. Dollimore, Thermochim. Acta 323 (1998) 75.
[22] K. Matusita, S. Sakka, Phys. Chem. Glass. 20 (1979) 81.
[23] K. Matusita, S. Sakka, J. Non-Cryst. Solids 38–39 (1980) 741.
[24] K. Matusita, T. Konatsu, R. Yokota, J. Mater. Sci. 19 (1984) 291.